https://dx.doi.org/10.22161/ijaers.6.3.9 ISSN: 2349-6495(P) | 2456-1908(O)

Evaluation of HadGEM2-ES and MIROC5 Models to simulate average Temperatures in the last Agricultural Frontier of the Brazilian Savannah

João Francisco S. Santos[1], Fernanda Alves Silva[1], Danuza Costa Leite[1], Danilo Ribeiro Barbacena[1], Liliana Pena Naval[2]

[1]Instituto Brasileiro de Geografia e Estatística, Unidade Estadual do Tocantins, Palmas, Brasil
[2]Programa de Pós-Graduação em Ciências do Ambiente, Universidade Federal do Tocantins, Brasil

***Abstract*— *The climate models adopted by the Intergovernmental Panel on Climate Change are capable of reproducing the current climate well on a continental scale, but need to be validated on a smaller scale. The objective of this study was to evaluate the performance of the regional models MarkSim-HadGEM2-ES and MarkSim-MIROC5 to estimate average temperatures in the last frontier of agricultural expansion of the Brazilian savannah. For this purpose, the data generated by the models were compared with those recorded by the National Institute of Meteorology and evaluated by statistical measures of correlation, bias and performance. The results revealed low bias and very good agreement, but high relative error and unsatisfactory performance in micro-regional and regional scales. Thus, the data generated by these models need correction to reproduce the current climate and enable reliable projections on these spatial scales.*

Keywords*— *evaluation, climate, modelling, savannah, temperature.

I. INTRODUCTION

The processes of climate change are part of the natural dynamics of the climate on the planet. However, the compilation of scientific studies conducted by the Intergovernmental Panel on Climate Change – IPCC (2014) attests to a probability above 95% that these changes are being accelerated and intensified by the increased concentration of greenhouse gases – GHGs coming mainly from the burning of fossil fuels and changes in land use and coverage to meet the growing needs of civilizations (Nkhonjera, 2017; Hsiang; Burke, 2014; IPCC, 2014; Marengo et al., 2011).

According to Broecker (2017), GHGs have increased their concentrations in the Earth's atmosphere to unprecedented levels since the beginning of the 20th century and, as a result, global warming has become unequivocal, affecting the evapotranspiration and precipitation system. In this sense, several researchers (O'Neill et al., 2017; Lesnikowski et al., 2015; Hsiang; Burke, 2014; IPCC, 2014; Huang et al., 2012; Marengo et al, 2012) state that the increase in average annual temperatures, at a global level, will increase the monthly and interannual variability of rainfall in many locations and these events, in turn, may generate various impacts on plantations and livestock, such as lack or excess of water, outbreaks of pests and diseases, flooding of productive lands, forest fires, among others that threaten the health and well-being of populations.

Climate change predictions are the result of scientific understanding of the interrelationships between the physical, chemical and biological processes that govern the functioning of the atmosphere, the oceans and the Earth's surface (Steinke, 2012; Riahi et al., 2011). This knowledge is used to create global climate models that estimate the future behaviour of rainfall, temperature, pressure, cloud cover, humidity and a series of other climate variables for a day, a month or a year (Riahi et al., 2011; Thomson et al., 2011). Currently, there are numerous climate models that integrate information on demographic and socio-economic trends in different temporal and spatial scales, but only seventeen of them were used in studies selected by phase five of the intercomparison of coupled models project – CMIP5 (Mach et al., 2016; IPCC, 2014). These models are considered the most reliable according to a set of criteria that include the effectiveness to reproduce the past and current climate within a given region, because if a model can perform simulations that are very similar to the known data, there is greater confidence that this model can project the future climate (Lewis. 2014; Moss, 2010). Therefore, the Global Climate Models – GCMs adopted by the IPCC (2014) are those that have demonstrated convincing ability to reproduce observed characteristics of the current climate and its changes in the past.

The GCMs provide reliable quantitative estimates of future climate change, particularly at continental scales in the order of 300 x 300 km (IPCC, 2014). However, the use of GCMs is limited in projecting climate change at the regional and sub-regional levels because significant differences in climate occur at a scale below the resolution of the GCMs. So, to expand the spatial resolution of the set of climate data produced by a GCM it is necessary to convert and validate them through downscaling methods (Silva, 2018; Lyra et al., 2017; Chou et al., 2012).

Feng et al. (2015) analysed ten models of the CMIP5 and demonstrated that none of them alone can capture long-term trends. This is due to a failure to simulate the difference between the interhemispheric sea surface temperature. Therefore, it is important to analyse the interannual variability of the simulations of the annual averages of the interesting variables in order to validate them through downscaling methods.

The need to validate the data generated in the downscaling process of a given GCM, through comparison with the data observed in different parts of the globe, makes it essential to select a period representative of local time to calculate a Climate Normal of interest (IPCC, 2013). A Climatic Normal (NC) is defined by the World Meteorological Organization (WMO, 2011) as the average of the atmospheric variables recorded in 30-year periods, starting on the first day of January of the years ending with digit one. For example, the average rainfall of a region in the period from January 1st, 1981 to December 31st, 2010 is an NC. However, the scarcity of meteorological records with such long historical series is a common problem in numerous regions of the planet. Therefore, the WMO (2011) recommends the adoption of the Provisional Climatological Normals (NCP) that should be calculated from periods of ten years of observations recorded data following the other criteria of the NC.

Among the models evaluated in CMIP5, MIROC5 (*Model for Interdisciplinary Research on Climate 5*) and HadGEM2-ES (*Hadley Centre Global Environmental Model 2 – Earth System*) are the ones that obtained the best results in simulating the present and past climate of South America (Lyra et al., 2017; Chou et al., 2012; Jones et al., 2011; Watanabe et al., 2011).

In the Brazilian savannah, the water cycle and temperatures are strongly influenced by vegetation characteristics (Strassburg et al., 2017), so it is highly vulnerable to global climate change. Therefore, the rapid expansion of natural areas converted into pastures and plantations can accelerate local climate change processes (Ayala et al., 2016; Imaflora, 2018).

The strategic importance of this biome for the preservation of the country's water resources is undeniable, since it absorbs and flows into it the waters that supply three important aquifers and six large Brazilian hydrographic basins, including the Amazon and the Tocantins. Additionally, this biome hosts large ecologically sensitive areas due to the great biodiversity of fauna and flora, with hundreds of endemic species and a mosaic of soils vulnerable to erosion and acidification processes (Strassburg et al., 2017; PBMC, 2014; Da Silva, 2013).

In this context, the objective of this study was to evaluate the performance of the simulations generated in the regional climate models MarkSim-HadGEM2-ES and MarkSim-MIROC5, based on data observed in conventional INMET weather stations located in the micro-regions that make up the last frontier of agricultural expansion of the Brazilian savannah.

II. MATERIAL AND METHODS

The territorial delimitation followed the proposal of Miranda et al. (2014) and was composed of 31 micro-regions of four federal units (UF) in Brazil, which encompass 139 municipalities in Tocantins, 135 in Maranhão, 33 in Piauí and 30 in Bahia distributed in an area of 73,848,967 hectares (Figure 1).

Fig. 1: Location of the study area.

This territory is composed predominantly of savannah formations (63.6%), but also presents transition areas between different types of flowers (15%) and seasonal forest (10.7%) on the borders with the Amazon biome and Caatinga to the west and east, respectively. The relief is characterized by large areas of slopes (39%) and depressions (56%), with altitudes ranging from 1 to

1200m above sea level. In the central extension, the semi-humid tropical climate is dominant and corresponds to about 78% of the territory, being characterized by periods of seven to eight months of scarce precipitation and average air temperature above 18°C in all the months of the year. On the eastern border, the semi-arid climate is characterised by the absence of rainfall for six months and high temperatures all year round. Four large hydrographic regions are contained within these limits, they are: Tocantins-Araguaia, Atlantic-North/Northeast stretch, Parnaíba and São Francisco (Magalhães et al., 2014; Mingonti et al., 2014).

The monthly averages of maximum, minimum and average temperatures were extracted from the records of the stations of the National Institute of Meteorology – INMET, available on the institution's website (http://www.inmet.gov.br/portal/).

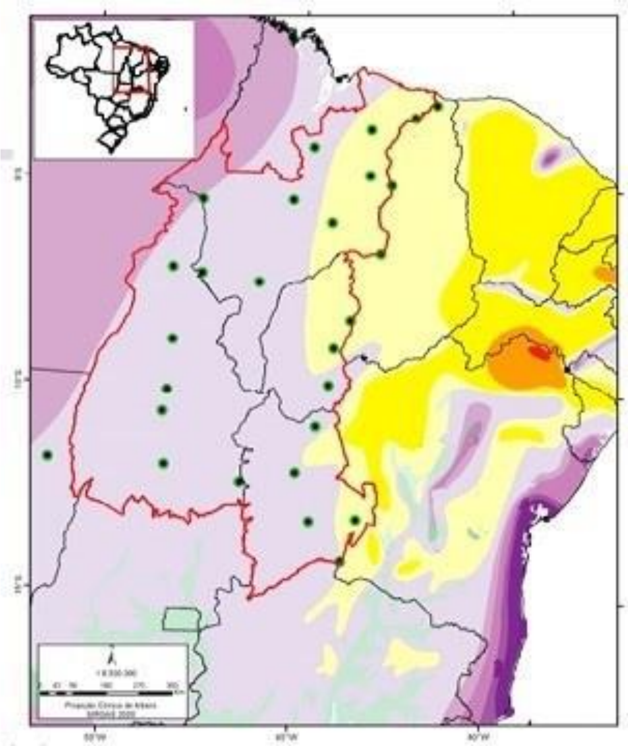

Fig. 2: Location of the 27 weather stations.

Historical records of observations made in 27 meteorological stations in the last ten years were used, referring to the period from January 2010 to December 2018. These records were associated with each micro-region (Table 1) which, according to information from the Municipal Agricultural Survey of the Brazilian Institute of Geography and Statistics (IBGE, 2018), has experienced an agricultural area growth of over 40% since 2009.

The daily climate data simulation was generated in the MarkSim-GCM. The MarkSim is a 3rd order Markov generator designed to estimate precipitation and daily temperatures that, according to Jones and Thornton (2013), has been used efficiently as a temporal and spatial downscaling, with resolutions up to 50 km (http://gisweb.ciat.cgiar.org/MarkSimGCM/). Therefore, temporal and spatial downscaling was used on the coordinates of the INMET stations from the HadGEM2-ES (*Hadley Centre Global Environmental Model 2 – Earth System*) models with resolution data of 1,2414°x1,875° (Jones et al., 2011) and MIROC5 (*Model for Interdisciplinary Research on Climate 5*) produced by the Climate System Research Center of the University of Tokyo, with resolution data of 1,4063°×1,4063° (Watanabe et al., 2010). Thus, data on precipitation, solar radiation and maximum and minimum temperatures were generated for the period from January 2010 to December 2018.

Table 1: Identification codes (ID) of the Micro-regions contained in the study area and their states.

Micro-region	ID	Micro-region	ID
Alto Mearim e Grajaú – MA¹	01	Cotegipe - BA	17
Alto Médio Gurguéia – PI²	02	Dianópolis - TO	18
Alto Parnaíba Piauiense - PI	03	Gerais de Balsas - MA	19
Araguaína – TO³	04	Gurupi - TO	20
Baixo Parnaíba Maranhense - MA	05	Imperatriz - MA	21
Barreiras – BA⁴	06	Itapecuru Mirim - MA	22
Bertolínia – PI	07	Jalapão - TO	23
Bico do Papagaio – TO	08	Lençóis Maranhenses - MA	24
Bom Jesus da Lapa – BA	09	Médio Mearim - MA	25
Caxias – MA	10	Miracema do Tocantins - TO	26
Chapadas das Mangabeiras - MA	11	Porto Franco - MA	27
Chapadas do Alto Itapecuru - MA	12	Porto Nacional - TO	28
Chapadas do Extremo Sul - PI	13	Presidente Dutra - MA	29
Chapadinha – MA	14	Rio Formoso - TO	30
Codó – MA	15	Sta Maria da Vitória - BA	31
Coelho Neto – MA	16		

States: Bahia⁴, Maranhão1, Piaui² e Tocantins³

https://dx.doi.org/10.22161/ijaers.6.3.9 ISSN: 2349-6495(P) | 2456-1908(O)

Descriptive statistics tools (mean, coefficient of variation, Student's t test and Pearson's correlation coefficient) were used in the *Paleontological Statistics Software Package for Education and Data Analysis* – PAST and used to analyse the results, adopting a significance level of 95% to test the possible interannual differences and relationships between the variables obtained and simulated.

To assess the accuracy of climate models, the percentage of bias (Pbias), mean absolute percentage error (EMPA) and mean absolute error (EMA) was used together with Willmott's agreement index (Willmott et al., 2012). On the other hand, the adapted performance index (C') of the models was evaluated by the product of Pearson's correlation coefficient (r) and Willmott's index (d), as proposed by Camargo and Sentelhas (1997).

The zero value for Pbias (Equation 1) indicates the absence of bias, while different values indicate overestimation, when negative, and underestimation, when positive (Van Liew et al., 2007). Considering that the observed data present a small margin of error, Pbias between -0.5% and +0.5% were considered null.

Equation 1:

$$P_{BIAS} = \left[\frac{\sum Obs_i - Est_i}{\sum Obs_i}\right] 100$$

Where:

Est_i – Estimated value of the variable for point *i*;

Obs_i – Observed value of the variable for point *i*.

The EMA measures the magnitude of the weighted average of absolute errors. For Willmott and Matsuura (2005), the EMA is a natural and more accurate measure of the mean magnitude of the error as can be seen in equation 2.

Equation 2:

$$EMA = \frac{1}{n}\sum_{i=1}^{n} |O_i - E_i|$$

Where:

E_i – Estimated value of the variable for point *i*;

O_i – Observed value of the variable for the point *i*;

n – Sample size.

The mean absolute percentage error – EMPA (Equation 3) is a precision statistic that prevents the error from being decreased by the sum of values with opposite signs and can be classified according to Table 2 (Lewis, 1997).

Equation 3:

$$EMPA = \frac{1}{n}\sum \left|\frac{Obs_i - Est_i}{Obs_i}\right| 100$$

Where:

Est_i – Estimated value of the variable for point *i*;

Obs_i – Observed value of the variable for point *i*;

n – Sample size.

Willmott's index reveals the degree of agreement between observed and simulated measurements, ranging from 0 to 1, where the first value represents the total disagreement and the second the perfect agreement. Thus, the higher the result of equation 4, the better the performance of the model.

Equation 4:

$$d = 1 - \frac{\sum_{i=1}^{n}(O_i - E_i)^2}{\sum_{i=1}^{n}(|E_i - \bar{O}| + |O_i - \bar{O}|)^2}$$

Where:

E_i – Estimated value of the variable for point *i*;

O_i – Observed value of the variable for the point *i*;

$\bar{O}$ – Average value of the observed variable

n – Sample size.

Table.2: Proposed classification for Pbias and performance index (C').

Pbias[1]	(C')[2]	EMPA[3]	Classification
<10%	> 0,75	< 10%	Very Good
10% - 14%	0,75 -0,64	10% - 19%	Good
15% - 24%	0,65 - 0,60	20% - 29%	Satisfactory
≥25%	< 0,60	≥30%	Unsatisfactory

[1]Van Liew et al. (2007); [2]Camargo e Sentelhas (1997); [3]Lewis (1997)

The adjustment of the models was performed by testing multiple regression models, and sinusoidal regression was selected because it better represents the cyclic regime of the temperature oscillations in the region.

III. RESULTS AND DISCUSSION

Figure 3 shows the behaviour of the quarterly averages of observed temperatures simulated by the HadGEM2-ES and MIROC5 climate models. The typical seasonality of the region (Lahsen et al., 2016; Curado et al., 2014) is satisfactorily reproduced in the model, but with a marked tendency to overestimate temperatures in the fourth quarter (October, November and December) and

https://dx.doi.org/10.22161/ijaers.6.3.9 ISSN: 2349-6495(P) | 2456-1908(O)

underestimate them in the second quarter (April, May and June). The same pattern of error was found, with small differences, in both models, and the largest errors recorded occurred in the second and third trimester, where the observed temperatures were much higher than those simulated. These quarters correspond to the post-harvest period in monoculture plantations, where the soil of large areas is uncovered and there is a sharp drop in air humidity due to low vegetation cover and, consequently, reduced evapotranspiration (Balduíno et al., 2018; Imaflora, 2018; Ayala et al., 2016; Curado et al., 2014; Da Silva, 2013).

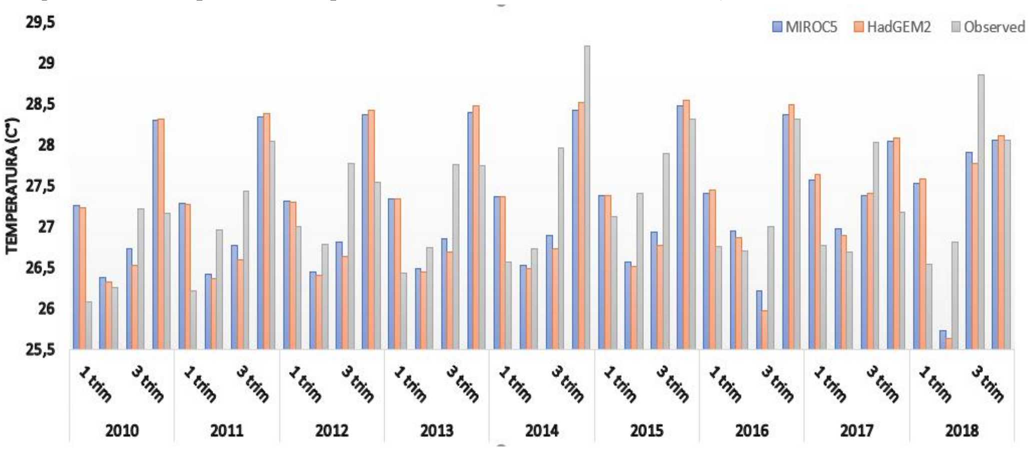

Fig. 3: Quarterly averages of Simulated and Observed Temperatures in the period from 2010 to 2018.

Table 3 presents the descriptive statistics of the simulated and observed data, on a monthly basis, in the studied area. It is possible to see that the models simulate measures of central tendency and interannual variability very similar to those observed, so that no significant difference between the variables was detected, at the minimum level of p≤0,05 in the Student's t test, in this time scale. There is also a low intra and interannual variability of mean temperature in this region, which according to Strassburg et al. (2017) represents an indication of greater vulnerability to environmental changes, since the functioning of almost all ecological services is adapted to low temperature ranges.

Table 3: Descriptive statistics of the studied period.

Statistical indicators	MIROC5	HadGEM2	Observed
Mean (C°)	27,267	27,231	27,277
Standard Deviation	1,012	1,104	0,950
Variation Coefficient (%)	3,710	4,056	3,481

Figure 4 shows the bias, or the absence of it, in the simulation of the two models in relation to the average monthly temperatures observed in each micro-region that presented expansion of agricultural areas in the last 10 years. This special view shows that the models provided overestimated data for most micro-regions.

The MIROC5 model had better results in this indicator, since it did not present bias in eight micro-regions (Fig 4B), while the HadGEM2-ES model did not have bias in only five micro-regions (Fig 4A). Five micro-regions had their temperatures underestimated in both models, being two central ones where savannahs predominate and three in the eastern border, in the transition from the Cerrado to the Semiarid. It is noticed that the absence of bias is concentrated in the micro-regions near the Amazon biome (IBGE, 2012), where there is also a higher frequency of classification divergence between the two models.

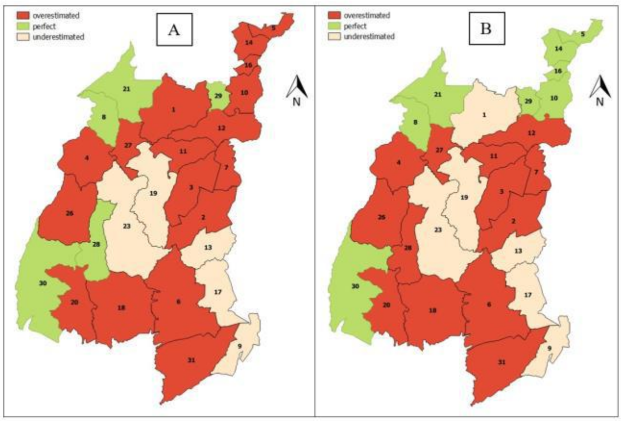

Fig. 4: Bias of over or underestimation of monthly mean temperatures in the simulations of the HadGEM2-ES (A) and MIROC5 (B) climate models in the period from 2010 to 2018.

Table 4 shows that the percentage of bias was classified as "very good" for both models and in all micro-regions analysed. However, it was found that in 11 micro-regions the HadGEM2-ES error is higher, while in other 10, the MIROC5 shows a higher error. For the others, the difference in errors between the two models is irrelevant. The same occurred with the Willmott index, with the

https://dx.doi.org/10.22161/ijaers.6.3.9 ISSN: 2349-6495(P) | 2456-1908(O)

smallest values located in micro-regions 02, 04, 17 and 18.

Average errors above 1.5ºC, in at least one of the models, were found in 33.3% of the micro-regions. It is noteworthy that, given the low variability (VC < 4.1%) of the interannual mean temperatures observed in the study area (Table 2) and in others (Batlle-Bayer et al., 2010; INPE, 2013), errors of this magnitude can be considered substantial, even though the agreement of the variables' behaviour is high (d>0.80). It was also observed that the MIROC5 model obtained greater errors than the HadGEM2-ES in most (57%) of the micro-regions.

Table 5 shows that the values obtained for each model in the statistical indicators, at a regional scale (study area unit), are similar in relation to precision (d), correlation (r) and the percentage of mean error (EMPA), these being classified as from moderate to very good. However, there are significant differences in relation to the bias (Pbias) and the performance indicator (C). Although the results of both models are classified as very good for the bias (Van Liew et al., 2007), they show unsatisfactory performance (Camargo and Sentelhas, 1997). In this sense, the MIROC5 model underestimates, while the HadGEM2 model overestimates the average temperatures. Both are considered very good, but the MIROC5 model is the one with the lowest bias. Part of these results are similar to those found by Sales et al. (2015). However, Torres (2014) also found many uncertainties in the validation of climate models, even with dynamic downscaling techniques.

Table 4: Model performance indicators in each micro-region of agricultural expansion.

ID	(d)		EMA		Pbias	
	Had	Miroc	Had	Miroc	Had	Miroc
1	0,94	0,92	1,22	1,35	-0,74	0,73
2	0,50	0,48	1,94	2,16	-3,54	-4,19
3	0,93	0,90	0,88	1,21	-1,41	-3,06
4	0,62	0,63	1,67	1,36	-5,64	-4,14
5	0,94	0,92	0,87	1,14	-1,25	0,00
6	0,83	0,89	0,71	0,95	-0,87	-2,17
7	0,94	0,92	1,29	1,39	-1,74	-0,56
8	0,93	0,94	1,15	1,04	0,25	0,20
9	0,83	0,88	1,43	1,12	1,15	0,54
10	0,96	0,94	1,13	1,27	-0,97	0,50
11	0,93	0,90	0,88	1,21	-1,41	-3,06
12	0,93	0,92	1,10	1,15	-2,26	-1,83
13	0,82	0,85	1,51	1,44	3,01	2,98
14	0,94	0,92	1,07	1,14	-1,25	0,00
16	0,94	0,92	0,97	1,14	-1,25	0,00
17	0,70	0,78	1,64	1,38	2,75	1,65
18	0,61	0,63	2,07	2,28	-3,64	-5,49
19	0,93	0,90	1,29	1,45	1,17	1,66
20	0,87	0,84	1,36	1,72	-4,02	-5,81
21	0,93	0,94	1,15	1,04	0,25	0,20
23	0,81	0,86	2,13	1,87	4,45	3,55
26	0,90	0,90	1,12	1,24	-3,17	-3,08
27	0,92	0,92	1,33	1,22	-1,40	-0,58
28	0,87	0,90	1,61	1,47	-0,01	-0,67
29	0,97	0,97	0,90	0,93	0,16	0,40
30	0,83	0,83	1,62	1,64	-0,01	-0,14
31	0,82	0,79	0,25	1,32	-1,34	-2,88

Table 5: Model performance indicators in relation to the total delimited area for the study.

Indicators	MIROC5	HadGEM2	Performance
(d)[1]	0,744	0,729	Very High
EMPA	3,054	3,079	Very Good
(r)[2]	0,526	0,561	Moderate
Pbias*	0,107	-0,854	Very Good
(C')*	0,392	0,409	Unsatisfactory

[1]Stork et al. (2016); [2]Levine et al. (2008); *significative ($p \leq 0,05$)

The analysis of the behaviour of the time series (Figure 2), composed by the observed data and estimated by downscaling of the models, revealed that the forecast errors present a cyclic pattern. Therefore, the adjustment of the models was performed by sinusoidal regression of four phases, that is, considering the averages of quarterly periods. The models were adjusted by Equation 5 and the coefficients generated for each model are expressed in Table 6.

Equation 5:

$$Y = (X_{max} - X_{min})*\cos(2\pi\,(X_i - X_{min})/(T - p))$$

Where:

Y – Adjusted estimated value;

X – Gross value estimated by the model.;

X_{max} – Estimated maximum gross value;

X_{min} – Estimated minimum gross value;

T – Estimation period;

p – Number of phase of the sinusoidal model.

Table 6: Sinusoidal adjustment coefficients.

	MIROC5		HadGEM2	
Phase	Range	Period	Range	Period
1	-0,697	3,590	-0,7572	3,673
2	-0,282	0,572	-0,3334	0,567
3	-0,447	0,152	0,3469	0,092
4	0,247	0,143	-0,3547	0,166

The adjustment results can be seen in Figure 5 and Table 7. It was confirmed that the adjustment generated an increase in agreement between the simulations and the observed data, which intensified the model's performance level and provided better temporal adjustments in the seasonal oscillations.

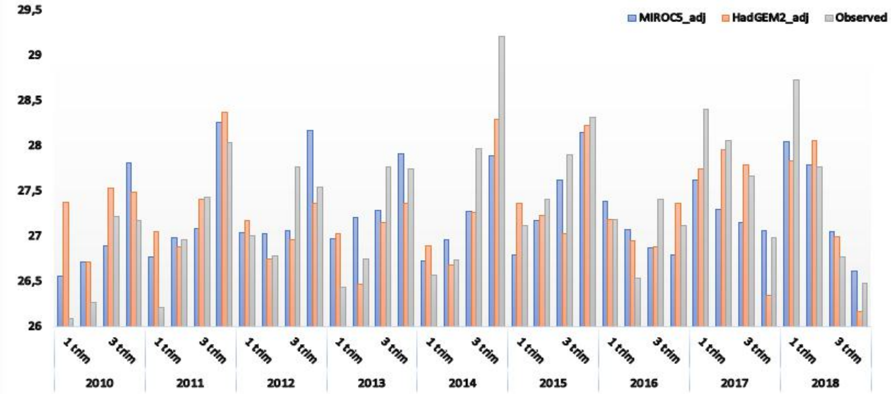

Fig. 5: Quarterly averages of Simulated and Observed Temperatures, with sinusoidal adjustment, throughout the studied period.

Table 7: Model performance indicators after sinusoidal adjustment.

Indicators	MIROC5	HadGEM2	Performance
(d)[1]	0,999	0,999	Very High
EMPA	1,976	1,997	Very Good
(r)[2]	0,50	0,52	Moderate
Pbias	0,002	-0,001	Very Good
(C')	0,707	0,721	Good

[1]Stork et al. (2016); [2]Levine et al. (2008).

IV. CONCLUSION

1 – Both models are accurate in reproducing the average annual and interannual temperatures, as well as their variability. However, they present difficulties in temporally synchronizing the typical monthly seasonality of the studied region, even though they reproduce them satisfactorily on an intra-annual scale;

2 – Both models present high levels of agreement in relation to the temperatures observed in the micro-regional scale, except in the micro-regions 02, 04, 17 and 18, where the level of agreement is classified as moderate;

3 – The bias of both models is less than 1% on a regional scale and varies from 0 to 5.64% on a micro-regional scale, being classified as "Very Good" in the two scales analysed. However, the models present biases in opposite directions in several micro-regions, and in the regional scale the MIROC5 tends to underestimate while the HadGEM2 tends to overestimate the interannual and micro-regional mean temperatures;

4 – The opposing biases in many micro-regions and in the studied region determined only a moderate correlation between the data simulated by both models in relation to the observed data. This affected the coefficient of performance of the models, which was classified as unsatisfactory in all spatial scales analysed;

5 – This is reinforced by the values presented in the mean absolute error, since, even with a reduced variability of intra- and interannual temperatures in all micro-regions, the error was higher than 1.5º C in several of them. Although the percentage of regional mean error was approximately 3%, the low variability of mean temperatures in the region makes this percentage high for the local reality, although classified in the literature as "very good";

6 – Despite the great balance in the performance of the two models, the MIROC5 was slightly higher on a regional scale. On the micro-regional scale, the superiority of one over the other is a result of the lowest bias and is divided similarly among micro-regions;

7 – Temperature simulation is important to estimate the other climate variables and make projections for the future (Balduíno et al., 2018; Bocchiola et al., 2013). Therefore, the results of this study show that the data generated in the regional climate models MarkSim-HadGEM2-ES and MarkSim-MIROC5 require correction of systematic errors prior to the use of future projections aimed at multiple objectives, especially in the planning of public policies that require greater intra-annual precision. However, for studies requiring only annual averages, it is sufficient to choose the model with the least bias in

micro-regional scales.

8 - The method of adjustment of the simulations, by means of sinusoidal regression, substantially increased the performance index of the estimates by improving the level of agreement between the simulated and observed data.

REFERENCES

[1] Ayala, L.M; Van Eupen, M; Zhang, G; Pérez-Soba, M; Martorano, L.G; Lisboa, L.S; Beltrao, N.E. Impact of agricultural expansion on water footprint in the Amazon under climate change scenarios. Science of the Total Environment, v. 570, p.1159–1173, 2016.

[2] Balduino, A. R; Santos, M. G ; Souza, L. B ; Lima, D. P ; Carvalho, A. P. Hydric balance and climatic classification of the city of Porto Nacional, state of Tocantins, inserted in the Legal Amazon, Brazil. International Journal of Advanced Engineering Research and Science , v. 5, p. 259-263, 2018.

[3] Batlle-Bayer, L; Batjes, N. H; Bindraban, P. S. Changes in organic carbon stocks upon land use conversion in Brazilian Cerrado. Agric. Ecosyst. Environ. 137 47–58, 2010.

[4] Bocchiola, D; Nana, E; Soncini, A. Impact of climate change scenarios on crop yield and water footprint of maize in the Po valley of Italy. Agric. Water Manager, v. 116, p. 50–61, 2013.

[5] Broecker, W. When climate change predictions are right for the wrong reasons. Climatic Change, v. 141, p. 1–6, 2017.

[6] Camargo, A. P; Sentelhas, P. C. Avaliação do desempenho de diferentes métodos de estimativas da evapotranspiração potencial no Estado de São Paulo, Brasil. Revista Brasileira de Agrometeorologia, Santa Maria, v.5, n.1, p.89-97, 1997.

[7] Chou, S. C.; Marengo, J. A.; Lyra, A. A.; Sueiro, G.; Pesquero, J. F.; Alves, L. M.; Kay, G.; Betts, R.; Chagas, D. J.; Gomes, J. L.; Bustamante, J. F.; Tavares, P. Downscaling of South America present climate driven by 4-member HadCM3 runs. Climate Dynamics, v. 38 n. 3-4, p. 635-653. 2012.

[8] Curado, L; Nogueira, J; Sanches, L; Rodrigues, T; Lobo, F; Bíudes, M. Inter Seasonality of the Energy Fluxes in Brazilian Savana-Mato Grosso-Brazil. Atmospheric and Climate Sciences, v. 4, p. 219-230, 2014.

[9] Da Silva, E. B. A dinâmica socioespacial e as mudanças na cobertura e uso da terra no bioma Cerrado. (Tese de Doutorado). Goiânia: Universidade Federal de Goiás, 2013.

[10] Feng, J.; Li, J.; Zhu, J.; Li, F.; Sun, C. Simulation of the equatorially asymmetric mode of the Hadley circulation in CMIP5 models. Adv. Atmos. Sci., v. 32, n. 8, p. 1129-1142, 2015.

[11] Hsiang, S.M.; Burke, M. Climate, Conflict, And Social Stability: What Does The Evidence Say? Climatic Change, v.123, p. 39–55, 2014.

[12] Huang, J.-B.; Wang, S.-W.; Luo, Y.; Zhao, Z.-C.; Wen, X.-Y. Debates on the causes of global warming. Adv. Clim.Change Res. v. 3, n. 1, p. 554-570, 2012.

[13] IBGE - Instituto Brasileiro de Geografia e Estatística. Pesquisa Agrícola Municipal 2018. Centro de Disseminação de Informações: IBGE, 2018.

[14] IBGE- Instituto Brasileiro de Geografia e Estatística. Mapa de Biomas do Brasil e o Mapa de Vegetação do Brasil. Rio de Janeiro: IBGE, 2012.

[15] IMAFLORA - Instituto De Manejo e Certificação Florestal e Agrícola. Evolução das emissões de gases de efeito estufa no Brasil (1990-2016): setor de mudanças de uso da terra. São Paulo: Observatório do Clima, 2018.

[16] IPCC - Intergovernmental Panel on Climate Change. Climate Change 2013: the Physical Science Basis Contribution of Working Group I to the Fifth Assessment Report. Cambridge: Cambridge University Press, 2013.

[17] IPCC - Intergovernmental Panel on Climate Change. WGII AR5: Climate Change 2014: Impacts, Adaptation, and Vulnerability: Summary for Policymakers, 2014.

[18] INPE - Instituto Nacional de Pesquisas Espaciais. Projeto TerraClass: Cerrado, 2013. Disponível em: http://www.dpi.inpe.br/tccerrado/. Acesso em: 12/03/2017.

[19] Jones, C. D.; Hughes, J. K.; Bellouin, N.; Hardiman, S. C.; Jones, G. S.; Knight, J.; Liddicoat, S.; O'connor, F. M.; Andres, R. J.; Bell, C.; Boo, K.-O.; Bozzo, A.; Butchart, N.; Cadule, P.; Corbin, K. D.; Doutriaux-Boucher, M.; Friedlingstein, P.; Gornall, J.; Gray, L.; Halloran, P. R.; Hurtt, G.; Ingram, W. J.; Lamarque, J.-F.; Law, R. M.; Meinshausen, M.; Osprey, S.; Palin, E. J.; Chini, L. P.; Raddatz, T.; Sanderson, M. G.; Sellar, A. A.; Schurer, A.; Valdes, P.; Wood, N.; Woodward, S.; Yoshioka, M.; Zerroukat, M. The HadGEM2-ES implementation of CMIP5 centennial simulations, Geosci. Model Dev., 4, 543-570, 2011.

[20] Jones, P.G.; Thornton, P.K. Generating downscaled weather data from a suite of climate models for agricultural modelling applications. Agricultural Systems, Amsterdam, v. 114,p. 1–5, 2013.

[21] Lahsen, M; Bustamante, M. M. C.; Dalla-Nora, E. L. Undervaluing and Overexploiting the Brazilian Cerrado at Our Peril, Environment: Science and

Policy for Sustainable Development, v. 58, n. 6, p. 4-15, 2016.

[22] Levine, D. M; Stephan, D. F; Krehbiel, T. C; Berenson, M. L. Estatística – teoria e aplicações. Rio de Janeiro: Livros técnicos e Científicos. 2008.

[23] Lesnikowski, A. C.; Ford, J. D.; Berrang-Ford, L.; Barrera, M.; Heymann, J. How are we adapting to climate change? A global assessment Mitig. Adapt. Strat. Glob. Change, v. 20 , p. 277–293, 2015.

[24] Lewis, K. Climate science in climate security scenarios. Climatic Change, v. 123, n. 1, p. 11–22, 2014.

[25] Lewis, C. D. **Demand Forecasting and Inventory Control**. A computer aided learning approach. Woodhead Publishing Ltd, 1997. p. 157.

[26] Lyra, A. A.; Tavares, P.; Chou, S. C.; Sueiro, G.; Dereczynski, C.; Sondermann, M.; Silva, A.; Marengo, J.; Giarolla, A. Climate change projections over three metropolitan regions in Southeast Brazil using the non-hydrostatic Eta regional climate model at 5-km resolution. Theoretical and Applied Climatology, v, 137, p. 11-22, 2017.

[27] Mach, K. J.; Mastrandrea, M. D.; Bilir, T. E.; Field, C. B. Understanding and responding to danger from climate change: the role of key risks in the IPCC AR5. Climatic Change, v. 136, p.427–444, 2016.

[28] Magalhães, L. A.; Miranda, E. E. de. A. de. Matopiba: Quadro Natural. Nota Técnica, Campinas, n. 5, 1-41, 2014.

[29] Marengo, J. A.; Chou, S. C.; Kay, G.; Alves, L. M.; Pesquero, J. F.; Soares, W. R.; Santos, D. C.; Lyra, A. A.; Sueiro, G.; Betts, R.; Chagas, D. J.; Gomes, J. L.; Bustamante, J. F.; Tavares, P. Development of regional future climate change scenarios in South America using the Eta CPTEC/HadCM3 climate change projections: Climatology and regional analyses for the Amazon, São Francisco and and the Parana River Basins. Climate Dynamics. v. 38, n 9, 1829-1848, 2012.

[30] Marengo, J. A.; Nobre, C. A.; Chou, S. C.; Tomasella, J.; Sampaio, G.; Alves, L. M.; Obregón, G. O.; Soares, W. R.; Betts, R.; Kay, G. (2011). Riscos das mudanças climáticas no Brasil: análise conjunta Brasil-Reino Unido sobre os impactos das mudanças climáticas e do desmatamento na Amazônia. Disponível em: <Disponível em: http://www.ccst.inpe.br >. Acesso em: 12set2018

[31] Mingnoti, R.; Brasco, M. A.; Holler, W. A.; Lovis Filho, E.; Spadotto, C. A. Matopiba: Caracterização das áreas com grande produção de culturas anuais. Embrapa Gestão Territorial - Nota Técnica, n.6,1-40, 2014.

[32] Miranda, E. E. de.; Magalhães, L. A.; Carvalho, C. A. de. Proposta de Delimitação Territorial do Matopiba. Nota Técnica, Campinas, n. 1, 1-18, 2014.

[33] Moss, R. H. The next generation of scenarios for climate change research and assessment. Nature, v. 463, n. 11, p. 747-756, 2010.

[34] Nkhonjera, G. K. Understanding the impact of climate change on the dwindling water resources of South Africa, focusing mainly on Olifants River basin: A review. Environmental Science & Policy, v. 71, p. 19-29, 2017.

[35] O'neill, B. C.; Oppenheimer, M.; Warren, R.; Hallegatte, S.; Kopp, R. E.; Pörtner, H. O.; Birkmann, J.; Foden, W.; Licker, R.; Mach, K. J.; Marbaix, P.; Mastrandrea, M. D.; Price, J.; Takahashi, K.; Van Ypersele, J.-P.; Yohe, G. IPCC reasons for concern regarding climate change risks. Nature Climate Change, v. 7, p. 28–37, 2017.

[36] PBMC - Painel Brasileiro de Mudanças Climáticas. Relatório do Painel Brasileiro de Mudanças Climáticas, 2014. Disponível em: <http://www.pbmc.coppe.ufrj.br/pt/publicacoes/relatorios-pbmc>. Acesso em: 22/05/2018.

[37] Riahi, K; Rao, S; Krey, V. RCP 8.5—A scenario of comparatively high greenhouse gas emissions. Climatic Change, v. 109, n. 1-2, Page 33, 2011.

[38] Sales, D.C.; Costa, A.A.; Silva, E.M.; VasconcelosJúnior, F.C.; Cavalcante, A.M.B.; Medeiros, S.S.; Marin, A.M.P.; Guimarães, S.O.; Araujo Junior, L.M.; Pereira, J.M.R. Projeções de mudanças na precipitação e temperatura no Nordeste Brasileiro utilizando a técnica de *downscaling* dinâmico. **Revista Brasileira de Meteorologia**, v. 30, n. 4, p. 435-456, 2015.

[39] Silva, R. A. Impacto das mudanças climáticas sobre a produtividade e Pegada hídrica da soja cultivada na região do MATOPIBA. Tese de doutorado em Meteorologia, Centro de Tecnologia e Recursos Naturais, Campina Grande: UFCG, 2018.

[40] Steinke, E.T. Climatologia fácil. São Paulo: Oficina de textos, 2012.

[41] Stork, l; Garcia, d. c; lopes, s. j; estefanel, v. Experimentação vegetal. Santa Maria: ed. UFSM, 2016.

[42] Strassburg, B.B.N; Brooks, T; Feltran-Barbieri, R; Iribarrem,A; Crouzeilles,R; Loyola,R; Latawiec, A.E; Oliveira Filho, F.J.B; Scaramuzza, C.A.M; Scarano, F.R; Soares-Filho, B; Balmford, A. Moment of truth for the Cerrado hotspot. Nature Ecology & Evolution, v. 1, n. 99, p. 1-3, 2017.

[43] Thomson, A. M; Calvin, K. V; Smith, S. J. RCP 4.5: a pathway for stabilization of radiative forcing by 2100. Climatic Change, v. 109, n.1-2, p. 7, 2011.

[44] Torres, R.R. Análise de incertezas em projeções de mudanças climáticas na América do Sul. Tese (Doutorado em Meteorologia) - Instituto Nacional de Pesquisas Espaciais, São José dos Campos: INPE, 2014.

[45] Van Liew, M. W.; Vieth, T. L.; Bosch, D. D.; Arnold, J. G. Suitability of SWAT for the Conservation effects assessment project: Comparison on USDA-agricultural research service watersheds. **Journal of Hydrologic Engineering**, v.12, n.2, p.173-189, mar. 2007.

[46] Watanabe, M.; Suzuki, T.; O'ishi, R.; Komuro, Y.; Watanabe, S.; Emori, S.; Takemura, T.; Chikira, M.; Ogura, T.; Sekiguchi, M.; Takata, K.; Yamazaki, D.; Yokohata, T.; Nozawa, T.; Hasumi, H.; Tetebe, H.; Kimoto, M. Improved climate simulation by MIROC5: mean states, variability, and climate sensitivity. **Journal of Climate**, v. 23, n. 23. p. 6312–6335, 2010.

[47] Watanabe, S.; Hajima, T.; Sudo, K.; Nagashima, T. Takemura, T.; Okajima, H.; Nozawa, T.; Kawase, H.; Abe, M.; Yokohata, T.; Ise, T.; Sato, H.; Kato, E.; Takata, K.; Emori, S.; Kawamiya, M. MIROC-ESM 2010: model description and basic results of CMIP5-20c3m experiments. Geoscientific Model Development. v. 4, p: 845–872, 2011.

[48] Willmott, C. J.; Robeson, S. M.; Matsuura, K. Short communication: A refined index of model performance. **International Journal of Climatology**, v. 32, p. 2088-2094, 2012.

[49] Willmott, C. J.; Matsuura, K. Advantages of the mean absolute error (MAE) over the root mean square error (RMSE) in assessing average model performance. Climate Research, v.30, p. 79–82, 2005.

[50] WMO- World Meteorological Organization. Guide to Climatological Practices n° 100. Secretariat of the, Geneva, WMO, 2011. https://library.wmo.int/pmb_ged/wmo_100_en.pdf